Water Research 242 (2023) 120213

Contents lists available at ScienceDirect

Water Research

journal homepage: www.elsevier.com/locate/watres

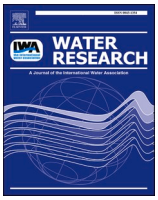

Global warming induces the succession of photosynthetic microbial communities in a glacial lake on the Tibetan Plateau

Jingwu Ouyang [a,1], Hongchen Wu [b,c,1], Huan Yang [a,*], Jingfu Wang [b,c,*], Jianbao Liu [d], Yindong Tong [e,f], Dengjun Wang [g], Miao Huang [a]

[a] Hubei Key Laboratory of Critical Zone Evolution, School of Geography and Information Engineering, China University of Geosciences, Wuhan, 430074, China
[b] State Key Laboratory of Environmental Geochemistry, Institute of Geochemistry, Chinese Academy of Sciences, Guiyang 550081, China
[c] University of Chinese Academy of Sciences, Beijing 100049, China
[d] Group of Alpine Paleoecology and Human Adaptation (ALPHA), State Key Laboratory of Tibetan Plateau Earth System, Resources and Environment (TPESRE), Institute of Tibetan Plateau Research, Chinese Academy of Sciences, Beijing 100101, China
[e] School of Environmental Science and Engineering, Tianjin University, Tianjin 300072, China
[f] College of Ecological Environment, Tibet University, Lasa 850000, China
[g] School of Fisheries, Aquaculture and Aquatic Sciences, Auburn University, Auburn, AL 36849, USA

ARTICLE INFO

Keywords:
Glacial lakes
Global warming
GDGTs
SedDNA
Tibetan plateau

ABSTRACT

As an important freshwater resource in the Qinghai-Tibet Plateau, glacial lakes are being immensely affected by global warming. Due to the lack of long-term monitoring data, the processes and driving mechanisms of the water ecology of these glacial lakes in a rapidly changing climate are poorly understood. This study, for the first time, reconstructed changes in water temperature and photosynthetic microbial communities over the past 200 years in Lake Basomtso, a glacial lake on the southeastern Tibetan Plateau. Temperatures were reconstructed using a paleotemperature proxy based on branched glycerol dialkyl glycerol tetraethers (brGDGTs), the cell membrane lipids of some bacteria, and photosynthetic microbial communities were determined by high-throughput DNA sequencing. The reconstructed mean annual air temperature (MAAT) at Lake Basomtso varied between 6.9 and 8.3 °C over the past 200 years, with a rapid warming rate of 0.25 °C /10 yrs after 1950s. Carbon isotope of sediment and *n*-alkane analyses indicate that ≥95% of the organic matter in Lake Basomtso is derived from a mixture of terrestrial C_3 plants and endogenous organic matter inputs, and the proportion of endogenous organic matter in the sediments has gradually increased since the 1960s. The sedimentary DNA analyses of the sediment core reveal that *Chloracea* is the most dominant prokaryotic photosynthetic microbial group (84.5%) over the past 200 years. However, the relative abundance of *Cyanobacteria* has increased from ≤6.8% before the 1960s to 15.5% nowadays, suggesting that warmer temperatures favor the growth of *Cyanobacteria* in glacial lakes. Among eukaryotic photosynthetic microorganisms, the *Chlorophyceae* have been gradually replaced by *Dinoflagellata* and *Diatomacae* since the 1980s, although the *Chlorophyceae* still had the highest average relative abundance overall (30–40%). The Pb isotopic composition, together with the total phosphorous concentration, implies that human activity exerted a minimal impact on Lake Basomtso over the past 200 yrs. However, the synchronous fluctuations of total organic carbon (TOC), total nitrogen (TN), and metal elements in sediments suggest that temperature appears to have a strong influence on nutrient input to Lake Basomtso by controlling glacial erosion. Global warming and the concurrent increase in glacial meltwater are two main factors driving changes in nutrient inputs from terrestrial sources which, in turn, increases the lake productivity, and changes microbial community composition. Our findings demonstrate the sensitive response of glacial lake ecology to global warming. It is necessary to strengthen the monitoring and research of glacial lake ecology on the Tibetan plateau, so as to more scientifically and accurately understand the response process and mechanism of the glacial lake ecosystem under global warming.

* Corresponding authors.
E-mail addresses: yanghuan37@cug.edu.cn (H. Yang), wangjingfu@vip.skleg.cn (J. Wang).
[1] Equal contribution.

https://doi.org/10.1016/j.watres.2023.120213
Received 8 April 2023; Received in revised form 8 June 2023; Accepted 9 June 2023
Available online 10 June 2023

1. Introduction

The Tibetan Plateau is famously entitled the "third pole" of the world and the "water tower of Asia"(Immerzeel et al., 2010), with a mean altitude of over 4000 m above the sea level and an overall area of about 2.5×10^6 km^2. Many important rivers fed by the glacier meltwater, such as the Yangtze River, Yellow River, Lancang River, and Nu River all originate from the Tibetan Plateau (Huo et al., 2022a). The glaciers on the Tibetan Plateau are estimated to cover an area of about 1×10^5 km^2 and the Tibetan Plateau has more than 1065 lakes with an area >1 km^2, among which more than 1/3 are glacial lakes (Yao et al., 2012; Tao et al., 2020). Glacial lakes are an important part of the freshwater resources of the Tibetan Plateau that play a crucial role in fueling the water system of the Tibetan Plateau.

Over the last few decades, the global surface has experienced significant warming, with the warming rate of the Tibetan Plateau at 0.44 °C/10 yr between 1980 and 2012, which is 2.75-folds with respect to the global average (0.16 °C/10 yr) (Xu et al., 2009; Lin et al., 2017; Huo et al., 2022a). Climate warming can cause changes in various hydrological processes and biogeochemical cycles of the water system on the Tibetan Plateau, which will likely adversely impact its ecological structure, function, and resilience (McLauchlan et al., 2013; O'Beirne et al., 2017). Multiple lines of evidence suggest that rapid warming is causing significant glacier recession on the Tibetan Plateau, with the loss of glacier stocks in the Asian Highlands accounting for ~19% of the total annual global loss of glacier stocks (267 ± 16 Giga ton (Gt)) from 2000 to 2019. This has caused a significant decline in terrestrial water resource reserves in the Asian Highlands (Hugonnet et al., 2021;Zhang et al., 2021a; Zhang et al., 2023b), and lake area increased from 38,596 km^2 to 46,831 km^2 (Tao et al., 2020; Tang et al., 2023). The glacial recharge to lakes on the Tibetan plateau increased by 127±14.3 Gt between 1976 and 2019, which is much higher than that (42.6 ± 4.9 Gt) of non-glacial lake water (Zhang et al., 2021b). The water quality of the Tibetan Plateau lake systems is currently acceptable, and ecological changes due to climate warming do not appear to have crossed the ecological threshold thus far (Wischnewski et al., 2011; Liu et al., 2021). However, field surveys of several lakes on the Tibetan Plateau have shown that climate change has caused significant impacts on lake biomes and ecosystems on the Tibetan Plateau through changing water salinity and temperature, resulting in variations of primary productivity and algal communities (Lin et al., 2017; Jia et al., 2022).

The water environment of glacial lakes on the Qinghai-Tibet Plateau (QTP) is vital for the livelihoods of local people and to the security of water resources in Asia. While previous studies on the physical characteristics and water quality changes of lakes on the QTP have provided useful information, a more comprehensive understanding of the evolution of the water environment and ecology in glacial lakes is a prerequisite for developing strategies for water resource protection. However, there is a paucity of studies on the long-term evolution of water quality and ecology in glacial lakes on the QTP over the past century.

Glacial lakes are one of the most sensitive while fragile areas to climate change with less resilience (Williamson et al., 2009; Zhu et al., 2020). For these unique attributes, glacial lake sediments are a good archive for documenting changes in water ecology and environment, which can be further used to reconstruct the long-term evolution of the lake water environment on the QTP. The lipid biomarker and sedimentary DNA (SedDNA) analyses in lake sediment cores have made it possible to reconstruct the long-term microbial community changes in lakes (Keck et al., 2020; Zhang et al., 2021b;Zhang et al., 2023a). For example, the evolution of the cyanobacterial community in Taihu Lake reconstructed by SedDNA revealed that increasing temperature and decreasing wind speed accounted for a gradual dominance of cyanobacteria in Lake Taihu (Zhang et al., 2023b). Multiple lipid biomarkers have been used to reconstruct changes in aquatic ecosystems, hydrology, and methane cycling in lake Wudalianchi from Changbai Mountain, China, before and after a regional volcanic eruption (Yao et al., 2022). These new methods, combined with the analyses of geochemical indicators such as nutrient elements and their isotopic compositions, can provide novel insights into the environmental changes and community evolution of aquatic ecosystems.

Herein, we employed lipid biomarkers and high-throughput DNA sequencing techniques to examine the evolution of the photosynthetic microbial community in a sediment core from Lake Basomtso, a glacial lake on the southeastern Tibetan Plateau. Temperature changes over the last 200 years were reconstructed using bacterial membrane lipids—branched glycerol dialkyl glycerol tetraethers (brGDGTs). Correspondingly, the input of exogenous organic matter and elements to lake sediments during this period were assessed using organic geochemical proxies and Pb isotopic compositions. Our findings provide strong data support to build a theoretical foundation for the development of strategies for water protection in glacial lakes on the QTP.

2. Material and method

2.1. Sampling

The Lake Basomtso (30°0′1″−30°2′53″N, 93°53′37″−94°1′48″E; 3500 m above the sea level) is a glacial-dammed freshwater lake located in the southeast of the Tibetan Plateau at the confluence of the Nyingchi Tanggula and the Himalayas. The lake has an area of about 26 km^2, and a maximum depth of about 120 m with a salinity of 0.12 g/L and water pH of 7.2 (Li et al., 2017). Its main source of recharge is via rainfall and glacier meltwater (Li et al., 2016). Lake Basomtso exhibits stratification characteristics during winter and summer. The low temperature, together with the hypoxic condition caused by water stratification, are favorable to the long-term preservation of organic matter and DNA within the sediments. Two parallel sediment cores of 44 cm and 52 cm in length respectively, with a clear sediment-water interface, were collected by a gravity corer from the center of the lake at a depth of 100 m (Fig. 1; 30°0′59″N, 93°55′54″E). The 52-cm sediment core was used for ^{210}Pb, ^{137}Cs, elemental content, and isotopic analysis, whereas the 44-cm sediment core was used to analyze lipids and DNA. The difference between the same proxies for the two sediment cores is expected to be minimal since we collected them at the same location. The cores were then split at 1 cm intervals. Sediment samples were stored in sealed 50 mL centrifuge tubes and samples were then freeze-dried at −80 °C.

2.2. Chronology

The sediment core was dated by excess ^{210}Pb (^{210}Pb$_{ex}$) and ^{137}Cs, which were analyzed using a multi-channel γ-ray spectrometer (GX6020, CANBERRA, USA) at the Institute of Geochemistry, Chinese Academy of Sciences. The ^{210}Pb activity was determined by γ-rays at 46.5 keV, while the ^{137}Cs activity was quantified by γ-rays at 662 keV. The ^{226}Ra activity was monitored by γ-rays emitted by its daughter isotope ^{214}Pb at 295 keV and 352 keV. Finally, the excess ^{210}Pb activity concentration (^{210}Pb$_{ex}$) was determined by subtracting the ^{226}Ra-supported ^{210}Pb activity (^{210}Pb$_{sup}$) from the measured total ^{210}Pb activity (Table S1). The absolute efficiency of the detector was determined using a calibrated source and a sediment sample of known activity, which was corrected for the self-absorption effect of low-energy γ rays within the samples.

The absolute ages of the sediment core were calculated using a constant flow and constant sedimentation rate (CFCS) model (Appleby and Oldfield, 1978). Given that the porosity of the sediment core decreases with depth, the cumulative mass depth (M; g cm^{-2}) was used instead of depth (cm) when calculating the sediment accumulation rates. The cumulative mass depth M(a) at depth a can be calculated using the formula (1):

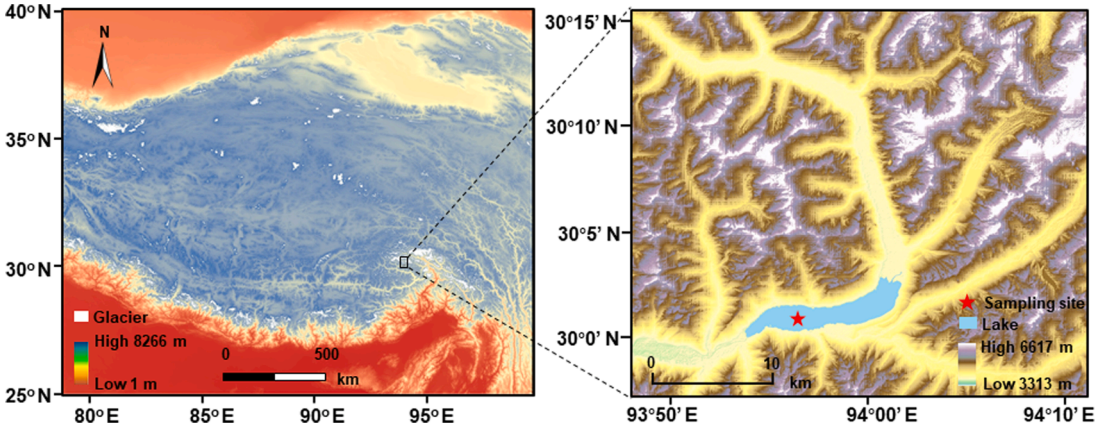

Fig. 1. A map showing a part of the Qinghai-Tibetan Plateau (QTP; left) and the location of the core sampling site in the Lake Basomtso (red star; right).

$$M(a) = \int_0^a \rho(z)dz \quad (1)$$

where ρ(*z*) is the dry bulk density of the sediment at depth *z* (Chen et al., 2019).

2.3. Determination of element concentrations and isotopic composition

Each sediment sample was immersed in 1 M HCl for 24 h to remove the carbonate and rinsed with Milli Q water until a neutral pH was reached. An aliquot of freeze-dried sediment was wrapped into a tin capsule. The elemental analyzer (Elementar Vario Macro cube, Germany) was used for total organic carbon (TOC) and total nitrogen (TN) analyses. An MAT 253 stable isotope ratio mass spectrometer (Thermo Fisher, USA) was used for $\delta^{13}C_{org}$ analysis. The $\delta^{13}C_{org}$ was calculated relative to the Vienna Pee Dee Belemnite (VPDB) standard, and for every 10 samples, a set of parallel samples ($n = 3$) was used to determine the reproducibility of results. Reproducibility for replicates was better than 1%, 4%, and 0.08% for TOC, TN, and $\delta^{13}C_{org}$ measurements, respectively.

The sediment was ashed for 2 h at 450 °C and extracted with 1 M HCl for 16 h. The total phosphorus (TP) concentrations were then determined using the molybdenum blue method, following Murphy and Riley (1962).

Fifty micrograms of each sediment sample were weighed in a Teflon container. HNO_3 and HF were then added and the sediment samples were digested at 180 °C for 36 h. After cooling back down to room temperature (25 °C), the mixture was evaporated to near dryness and redissolved in HNO_3. The solvent was evaporated again. 2 mL of 14 M HNO_3 and 3 mL of Milli-Q water were added to the sample and metal elements in the digested samples were extracted at 150 °C for 24 hrs. Samples were diluted and the major and trace element concentrations were determined by ICP-OES (Inductive-Coupled Plasma Optical Emission Spectrometer, Vista-MPX, Varian, USA) and ICP-MS (Inductively Coupled Plasma Mass Spectrometer; 7700x, Agilent, USA) respectively. Quality control was performed with blank samples, and standard reference material (GBW07557). The reproducibility of duplicate samples was better than 5% for all elements except Cd (< 18%).

To determine the source of metal elements, Pb isotopic compositions were determined by multi-receiver ICP-MS (Nu Plasma II, Thermo Fisher Scientific, USA). An aliquot of sediment samples was digested with HCl (12 M), HNO_3 (16 M), and HF(22.6 M) at 180 °C for 36 h. After evaporation, the samples were then redissolved with a mixture of 2 M HCl and 1 M HBr (2:1, v/v). Pb was separated using an ion exchange resin (Dowex-1 × 8) and Thallium (Tl) was added before measurement to improve accuracy (Reuer et al., 2003). Except for HBr, other acids in the experiments were twice distilled and purified by an anionic resin (Dowex-1 × 8) in a Class 1000 ultra-clean room. The isotope standard reference material (NIST SRM 981) and three parallel samples ($n = 3$) were analyzed to monitor instrumental signal drift and mass bias. The results showed that the relative deviations of $^{208}/^{206}Pb$ and $^{206}/^{207}Pb$ for NIST-SRM 981 were both less than 0.1%, and the reproducibility of the $^{208}/^{206}Pb$ and $^{206}/^{207}Pb$ duplicate samples was better than 0.1% and 0.15%, respectively.

2.4. Lipid analysis

Lipids in the sediment samples were extracted with a mixture of dichloromethane (DCM) and methanol (MeOH) (9:1, *v/v*). The mixture was centrifuged, and the resulting supernatant was transferred to a flask containing copper for removing sulfur. The total lipid extracts (TLEs) were separated on a silica gel column into non-polar (alkanes) and polar fractions (GDGTs) by eluting with *n*-hexane and DCM: MeOH(1:1,v/v), respectively.

The non-polar fractions were analyzed by using gas chromatography (GC-FID 2010, Shimadazu, Japan) equipped with a DB-5 column. Cholestane was used as an internal standard. The high-purity H_2 gas was used as the carrier gas. The GC was initially operated at 70 °C, ramped up to 210 °C at 10 °C/min, and then to 300 °C at 3 °C/min. The *n*-alkanes with a carbon number ranging from C_{15} to C_{33} were quantified according to peak area and internal standard.

The polar fraction was re-dissolved in 300 μL of *n*-hexane/isopropanol (99:1, v/v) mixture. GDGTs were analyzed by high-performance liquid chromatography-atmospheric pressure chemical ionization-mass spectrometry (Agilent 1200 HPLC-APCI-6460A MS/MS). Two Hilic silica columns (Waters, USA) in sequence were used to separate GDGTs and maintained at 40 °C throughout the analysis. The elution gradient was used: 82% A/18% B isocratically for the first 25 min, 82% to 65% A for another 25 min, 65% to 0% A for the following 30 min, and A back to 82% in 10 min, where $A = n$-hexane and $B = n$-hexane: isopropanol (9:1, *v/v*)(Hopmans et al., 2016). The protonated ions of GDGTs ($[M + H]^+$) were scanned in single ion scanning mode (SIM) targeting mass-to-charge ratios (*m/z*) of 1302, 1300, 1298, 1296, 1292, 1050, 1048, 1046, 1036, 1034, 1032, 1022, 1020, 1018, 653 and 744. C_{46} GTGTs were used as an internal standard.

2.5. DNA analysis

SedDNA for each sediment core sample was extracted using DNA isolation kits (Hangzhou Bioer Technology Co.,Ltd, China) following the manufacturer's protocol. The Cat. Number of DNA isolation kit is BSC48L1E-G. The purity and concentration of DNA were determined using a Nanodrop One spectrophotometer (Thermo Fisher Scientific,

MA, USA). Eukaryotic universal primers 960F (5′-GGCTTAATTTGACTCAACRCG-3′) and NSR1438 (5′-GGGCATCACA GACCTGTTAT-3′) were used to amplify the highly variable V7 region of the 18S rRNA gene (Gast et al., 2004; Van de Peer et al., 2000), and cyanobacteria-specific primers CYA359-F, 5′-GGGGAATYTTCCGCAATGGG-3′, and CYA784-R, 5′-ACTACWGGGGTATCTAATCCC-3′ were used for amplification of the highly variable V3-V4 region of 16S rRNA (Nübel et al., 1997).

Polymerase Chain Reaction (PCR), containing 25 μL 2× Premix Taq (Takara Biotechnology, Dalian Co. Ltd., China), 1 μL of 10 μM each primer, and 3 μL of 20 ng/μL DNA template in a volume of 50 μL, were amplified by thermocycling: initial denaturation at 94 °C for 5 min, followed by 30 cycles of 30 s at 94 °C, 30 s at 52 °C, and 30 s at 72 °C, and a final extension at 72 °C for 10 min. The length and concentration of PCR products were detected by 1% agarose gel electrophoresis. The PCR products were purified by E.Z.N.A. ® Gel Extraction Kit (Omega, USA).

Sequencing libraries were generated using NEBNext® Ultra™ II DNA Library Prep Kit for Illumina® (New England Biolabs, MA, USA) as per the manufacturer's recommendations and index codes were added. The amplicons were sequenced on an Illumina Nova 6000 platform and 250 bp paired-end reads were generated (Guangdong Magigene Biotechnology Co., Ltd. Guangzhou, China). The sequences were trimmed and filtered using Qiime software (version 1.7.0). The final sequences were clustered at 97% similarity using usearch software as the operational taxonomic units (OTUs).

2.6. Paleotemperature reconstruction

Bacterial membrane lipids–brGDGTs are emerging tools for paleotemperature reconstruction in lakes (Tierney et al., 2010). BrGDGTs are named with Roman numerals I, II, and III, which correspond to 4, 5, and 6 methyl groups on the alkyl chains of brGDGTs, respectively; The lowercase a, b, and c denote 0, 1, and 2 cyclopentyl rings on the alkyl chains of brGDGTs, respectively. In addition, the ′ (prime) symbol is used to indicate the isomers with the methyl moiety at the C_6 position instead of the C_5 position (De Jonge et al., 2013). The distribution of 15 brGDGT compounds in global lake sediments was found to be closely related to mean annual air temperature (MAAT) (Martínez-Sosa et al., 2021) and has been widely used to infer past temperature variation (Feng et al., 2019; Martin et al., 2020).

To reconstruct the paleotemperature in the sediment core of Lake Basomtso, we first collected the instrumental mean annual air temperature (MAAT) data from 1961 to 2018 at the meteorological station in Bayi Town, which is 2992 m above sea level and 60.1 km from Lake Basomtso. Based on the dating results of the core, the distribution of brGDGTs in the top sediments of the core over the period of 1961–2018 was used to develop a lake-specific calibration for temperature reconstructions in Lake Basomtso. Stepwise forward selection (SFS), a statistical method to select the brGDGT compounds that have the most significant correlation with temperature over the period of 1961–2018, was employed and a brGDGT calibration for temperature reconstruction was obtained:

$$\mathrm{MAAT} = 2.5 \times f(\mathrm{IIa}') + 4.81 \left(R^2 = 0.79, p < 0.05\right) \quad (2)$$

where f(IIa′) is the relative abundance of IIa′ in all brGDGTs.

Temperature before the year 1961 in the sediment core was reconstructed using this calibration.

2.7. Vegetation type reconstruction

The Average Carbon chain Length (ACL) and aquatic vegetation index (P_{aq}) of long-chain *n*-alkanes (carbon chain > 21) were calculated respectively using the *n*-alkane abundance in the sediments (Ficken et al., 2000; Poynter et al., 1989) according to the formula as follows:

$$\mathrm{ACL} = \left(\sum i * C_i\right) \Big/ \sum C_i \quad (3)$$

$$P_{aq} = (C_{23} + C_{25}) / (C_{23} + C_{25} + C_{29} + C_{31}) \quad (4)$$

where i denotes the carbon chain length over the range from 23 to 33 and C_i denotes the relative abundance of *n*-alkanes with carbon chain length i. Higher ACL and lower P_{aq} values indicate more contribution of terrestrial higher plants and emergent macrophytes than submerged/floating plants to the organic matter pool in the lake sediment core (Ficken et al., 2000).

2.8. Assessment of heavy metal pollution degree

The enrichment factor (EF) was used to evaluate the extent of heavy metal contamination and the EF is calculated as follows:

$$\mathrm{EF} = (T_S / R_S) / (T_b / R_b) \quad (5)$$

where T_s and T_b represent targeted metal element concentrations in sediment samples and background, respectively; R_s and R_b represent reference element concentrations in sediment samples and background, respectively. The concentration data at the bottom of the sediment column core (>34 cm) was selected as the background, and the rock-forming element aluminum (Al) was selected as the reference element.

3. Results and discussion

3.1. Chronology

The $^{210}Pb_{ex}$ decreases logarithmically with increasing mass depth and gradually converges to background values at the bottom of the sediment core (Fig. 2). Due to the large uncertainty of $^{210}Pb_{ex}$ in the lower part of the sediment core, only data collected from < 22 cm depth were used to calculate lake sediment ages through the CFCS model (Appleby and Oldfield, 1978; Zhan et al., 2019). While this may lead to greater dating uncertainty in the lower part of the sediment core, it does not affect the main conclusions, because the variation of $^{210}Pb_{ex}$ and ^{137}Cs in the sediment core was primarily found in the middle and upper parts of the sediment core.

The CFCS model for $^{210}Pb_{ex}$ shows an average deposition rate of approximately 0.15 g/(cm^2·yr) in Lake Basomtso, and the calculated age based on the CFCS model shows the age of 1966 occurs at 13 cm. The maximum peak of ^{137}Cs occurs at 13 cm depth, corresponding to 1963. The age discrepancy between the ^{137}Cs and CFCS model is minor (3 yrs) and indicates that the dating results are reliable.

3.2. Temperature variation over the last 200 yrs

The MAAT change over the last 200 years reconstructed from brGDGTs in the sediment core of Lake Basomtso is shown in Fig. 3. Instrumental temperature data from the weather station in Bayi, a town near Lake Basomtso, shows that MAAT in the region increased between 1961 and 2018 and ranged from 6.5 to 9 °C, with an average of 7.7 °C. The MAAT reconstructed from brGDGTs also shows an increasing trend during the period, with temperature variations ranging from 7.2 to 8.2 °C, with an average of 7.7 °C. Overall, the reconstructed MAAT matched significantly well with the instrumental data ($R^2 = 0.79, p < 0.05$)(Fig. S3), indicating that the reconstructed temperature record was reliable.

Over the past 200 years, the variation of MAAT in Lake Basomtso ranged from 6.9 to 8.3 °C (Fig. 3), with an average of 7.5 °C. Before 1930, MAAT at Lake Basomtso showed no clear trend, with temperatures fluctuating between 7.2 and 8.1 °C (averaged at 7.4 °C). Between 1930 and 1960, temperatures fell from 7.8 °C to 6.9 °C but then increased rapidly to 7.9 °C. Subsequently, the MAAT showed a continuously increasing trend, and remaining above 8 °C for almost 20 years.

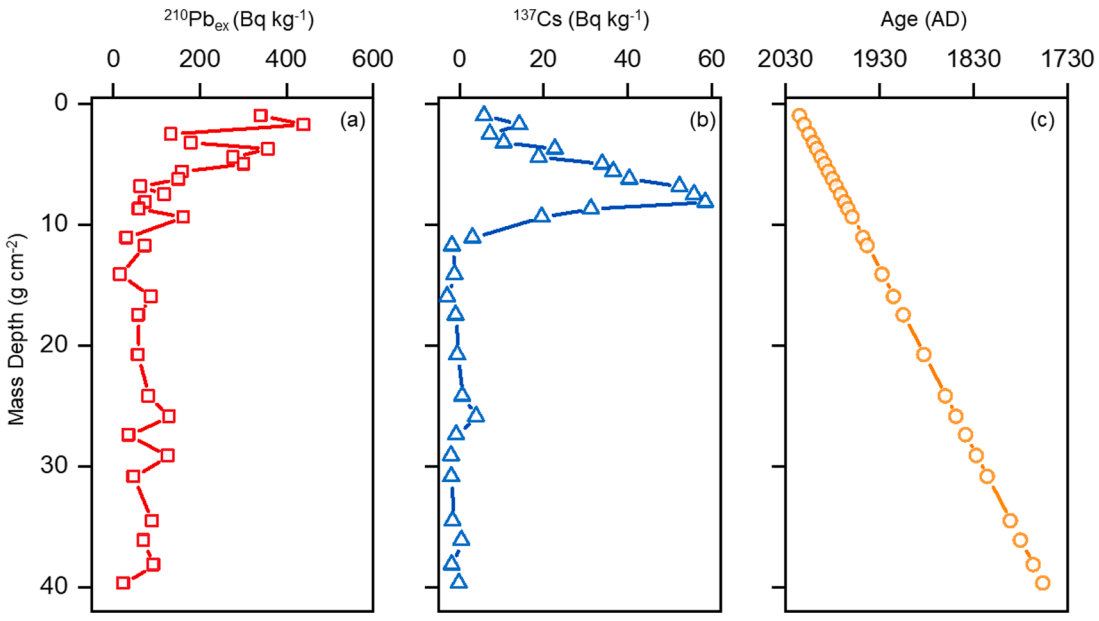

Fig. 2. $^{210}Pb_{ex}$ (a) and ^{137}Cs (b) activity-mass depth profiles and the chronology (c) in the sediment core of Lake Basomtso.

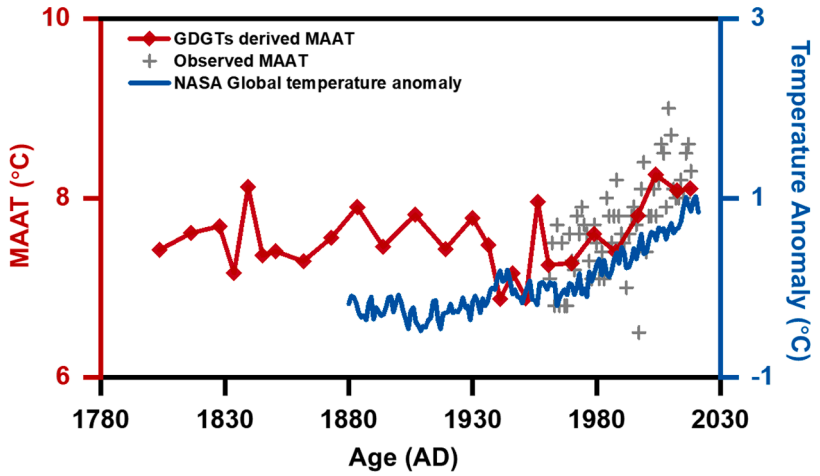

Fig. 3. Temporal variations of the brGDGT-derived MAAT in the Lake Basomtso, the observed MAAT in Bayi station, and the NASA global temperature anomaly compared to the long-term average from 1951 to 1980 (https://climate.nasa.gov/vital-signs/global-temperature/).

Compared to global temperature trends, temperature trends at Lake Basomtso are more significant (Fig. 3), especially during the post-1950 period. Global temperatures have increased by about 0.9 °C since 1950. In contrast, the temperature at Lake Basomtso increased by around 1.2 °C, which is significantly higher than the global average, mainly due to the higher altitude of Lake Basomtso. The rate of surface temperature rise is usually higher on plateaus than that at lower altitudes, due to a combination of surface reflection, cloud radiation, surface water vapor, and radiative flux changes (Pepin et al., 2015; Tang et al., 2023).

3.3. Temporal changes in historical primary productivity

TOC, TN, and TP contents in Lake Basomtso sediments ranged from 0.26 to 0.83%, 0.026 to 0.065%, and 0.063 to 0.073%, respectively (Fig. 4). Before 1930, TOC, TN, and TP contents showed no obvious change, fluctuating around 0.59%, 0.039%, and 0.069%, respectively. From 1930 to 1950, TOC, TN, and TP contents dropped rapidly to 0.26%, 0.03%, and 0.063%, respectively. However, TOC, TN, and TP contents quickly rebounded to 0.64%, 0.05%, and 0.073%, respectively, from 1950 to 1960. After 1960, TOC and TN contents continued to rise, while TP content showed a downward trend. In general, TOC and TN contents exhibit similar trends to our reconstructed temperature, suggesting that temperature has a significant influence on organic matter accumulation in Lake Basomtso sediments (Figs. 3 and 4). However, TP content displays an opposite trend to temperature since 1960. This decline in TP content is likely attributed to the reduction in the phosphorus content of catchment soils. In recent years, excessive grazing and climate change have contributed to the degradation of pastures on the Tibet Plateau (Dong et al., 2016; Ren et al., 2013), resulting in a reduction in the phosphorus content of the top soils. Consequently, there has been a decrease in the phosphorus input into the lake through surface runoff, which has resulted in a gradual decline in sediment TP contents.

The organic carbon isotope ($\delta^{13}C_{org}$), ACL, and P_{aq} were used to identify the source of organic matter. In general, photosynthetic microorganisms in the lake water and higher plants in the lake catchment are the two main sources of organic matter in the lake sediments

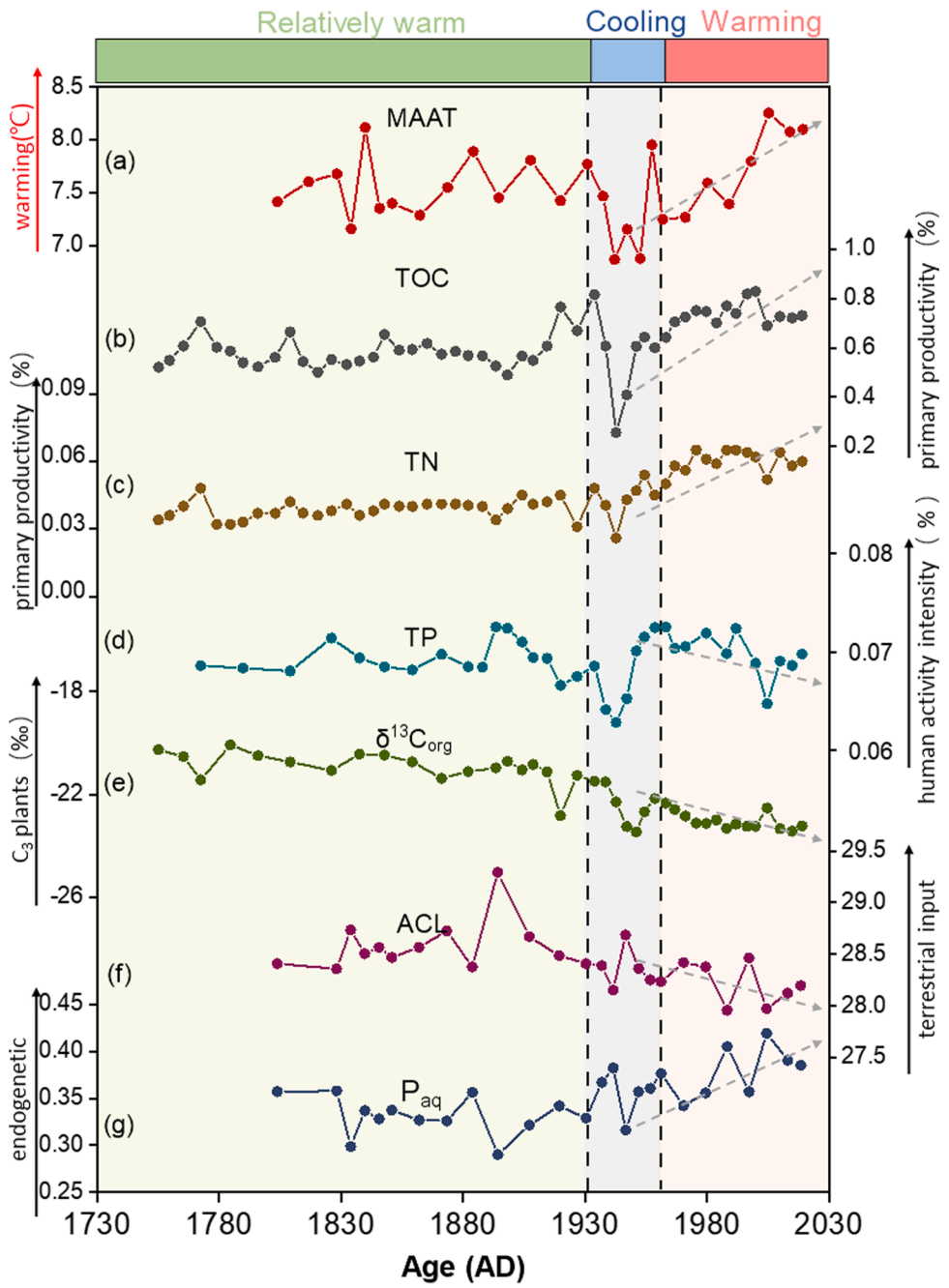

Fig. 4. Temporal variations of MAAT (a) with TOC (b), TN (c), TP (d), $\delta^{13}C_{org}$(e), ACL (f), and P_{aq} (g) over the past 200 yrs in the Lake Basomtso.

(Pinckney et al., 2001). C_3 plants are reported to have a lower $\delta^{13}C_{org}$, typically ranging from −24‰ to −30‰, whereas C_4 plants have a relatively higher $\delta^{13}C_{org}$ (−10‰ to −16‰), the $\delta^{13}C_{org}$ value of organic matter from photosynthetic living microorganisms in the lake is close to that of the C_3 plants (Meyers, 2003; Lu et al., 2020). Higher ACL values indicate a higher organic matter input from terrestrial higher plants, while lower ACL values indicate an increased input of endogenous organic matter (Li et al., 2022). P_{aq} is an indicator of the proportion of submerged plants/phytoplankton relative to terrestrial vegetation inputs, lower P_{aq} indicates inputs of terrestrial organic matter, while higher P_{aq} indicates inputs of organic matter from internal phytoplankton or submerged plants (Ficken et al., 2000).

The $\delta^{13}C_{org}$, ACL, and P_{aq} of the Lake Basomtso sediments vary from −23.5‰ to 20.1‰, 28.0 to 29.3, and 0.29 to 0.42, respectively. Together, these proxies indicate that organic matter in Lake Basomtso is mainly derived from terrestrial C_3 plants with mixed inputs like endogenous organic matter from the lake. Before 1930, these proxies were relatively stable, but after 1930, the $\delta^{13}C_{org}$ of Lake Basomtso sediments gradually decreased while ACL slightly decreased and P_{aq} showed an increasing trend (Fig. 4). These findings indicate that the proportion of endogenous organic matter in Lake Basomtso sediments gradually increased, and the primary productivity within the lake continuously enhanced.

The rise in the primary productivity of lakes in the modern period is mainly due to the increased anthropogenic nutrient inputs and climate change (Monchamp et al., 2018). However, with the rapid development of tourism in Lake Basomtso since the 1980s, human activity is in a constant state of enhancement, but overall, the impact of human activity on the environment of Lake Basomtso is still very weak. To better assess the impact of human activities on Lake Basomtso, we analyzed the

sedimentary heavy element concentrations. The results showed consistency between the concentrations of heavy elements (Fig. S1a) and the historical changes in TOC and TN contents, both of which responded well to temperature changes. The increase in temperature led to an increase in glacial meltwater and more nutrients entered the lake along with the meltwater that fuels more nutrients to the microbial community. At the same time, the biological communities within the lakes are more active, yielding higher primary productivity of the lakes.

While TP content followed the same trend as temperature before 1960, it showed a decreasing trend after 1960. This indicates that the flourishing of photosynthetic microorganisms was not related to the increase in TP, and human activities had no significant effect on the photosynthetic microbial community of the lake, by analyzing the heavy metals in Lake Basomtso, we found that the EF of these metals all fluctuated around 1 (Fig. S1b), suggesting that they are more likely associated with natural origin (Kang et al., 2017). The Pb isotope data further suggest the weak influence of human activities on Lake Basomtso. As shown in Fig. S2, the $^{208}Pb/^{206}Pb$ and $^{206}Pb/^{207}Pb$ values range from 2.081 to 2.087 and from 1.197 to 1.204, respectively, for Lake Basomtso sediments. These isotopic values differ significantly from typical anthropogenic Pb from vehicle exhaust, coal combustion, and metal smelting (Zheng et al., 2004), and are also inconsistent with the atmospheric Pb isotopic composition of major cities in South and East Asia (Mukai et al., 2001). In contrast, the Pb isotopes of the Lake Basomtso sediments are closer to the natural end members such as desert dust and loess (Ferrat et al., 2012), which fall within the riverine sediment range of the Tibetan Plateau (Tan et al., 2014). Therefore, climate warming, rather than human activity, is the main driver for the rise in primary productivity in Basomtso Lake.

3.4. Temporal succession of photosynthetic microbial communities

High-throughput sequencing of SedaDNA provides an effective strategy to assess long-term trends in photosynthetic microbial communities. A total of 1463,060 and 1548,670 prokaryotic and eukaryotic rRNA gene sequences were obtained from 22 Lake Basomtso sediment samples, containing 5698 prokaryotic and 2276 eukaryotic OTUs. The final results include 2229 prokaryotic and 152,784 eukaryotic photosynthetic microbial reads, clustered in 69 prokaryotic and 182 eukaryotic photosynthetic OTUs, respectively. The absolute abundance of eukaryotic and prokaryotic organisms responded better to temperature. To reduce the effect of DNA degradation, relative abundance was used to further explore the sequence of temporal changes in the photosynthetic microbial community (Fig. 6). The relative abundance was calculated as the proportion of a particular prokaryotic/eukaryotic photosynthetic microbe to the total prokaryotic/eukaryotic photosynthetic microbes to better represent the variation in different photosynthetic microbial communities.

As shown in Fig. 5, the Chao index of α diversity exhibits a generally increasing trend for both prokaryotic and eukaryotic microorganisms from 1800 onward. Especially, there is a significant rising trend since the 1960s, which is slightly higher than the average global warming rate. These observations indicate that temperature is an important control on biodiversity in Lake Basomtso and that temperature change has a dramatic effect on the biological communities in the lake.

In terms of the microbial communities, a total of two prokaryotic photosynthetic microorganisms, *Cyanobacteria* and *Chloracea*, were detected in the Lake Basomtso sediments as shown in Fig. 6. In all sediment samples, *Chloracea* was the most dominant prokaryotic photosynthetic microorganism with average relative abundance of 90.6%, while *Cyanobacteria* had an average relative abundance of only 9.4%. The eukaryotic photosynthetic microorganisms detected included *Chlorophyceae* (25.6%), *Dinoflagellata* (22.9%), *Diatomacae* (19.3%), *Trebouxiophyceae* (14.9%), *Chrysophyceae* (11.6%), and *Eustigmatophyceae* (5.8%) (Fig. 6).

With respect to the historical trends, the relative abundance of *Cyanobacteria* has increased significantly since 1960, although *Chloracea* remains the dominant prokaryotic photosynthetic microbial community. In the latest 40 years, the average relative abundance of *Cyanobacteria* has reached 15.5%, much higher than the average relative abundance before 1980 (7.1%). Similarly, changes in photosynthetic microbial communities have been observed for eukaryotic photosynthetic microorganisms: although *Chlorophyceae* had the highest mean relative abundance (29.5%), *Dinoflagellata* and *Diatomacae* began to rise rapidly after 1960, and after 1980, *Chlorophyceae* began to gradually increase. More importantly, *Dinoflagellata* and *Diatomacae* became the dominant eukaryotic photosynthetic microorganisms in the present-day sediments of Lake Basomtso. Often, *Cyanobacteria* flourish best in water bodies at 25–35 °C, while *Dinoflagellata* and *Diatomacae* also tend to dominate towards warmer environments with a stronger competitive advantage in warmer climates (Watson et al., 1997). Although MAAT in Lake Basomtso region is below 10 °C, temperatures have risen rapidly

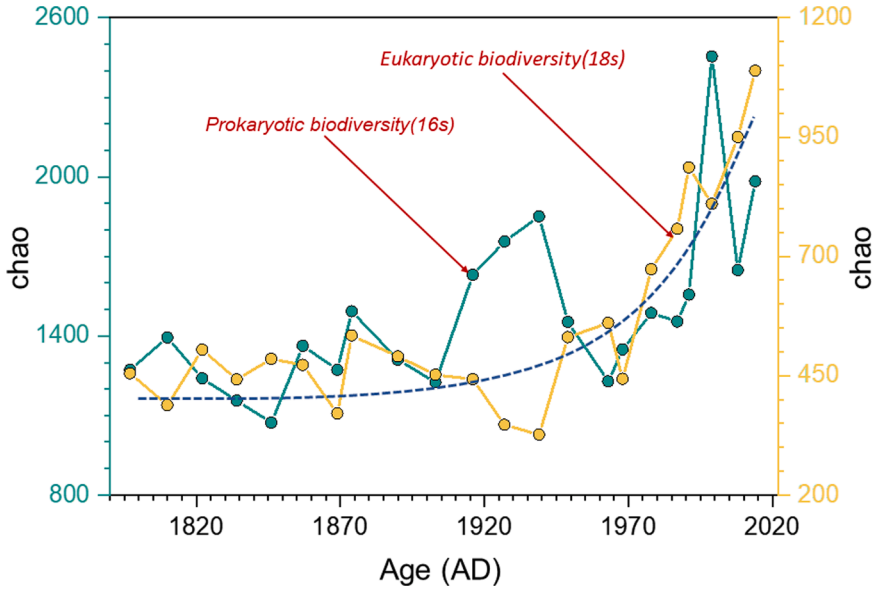

Fig. 5. The bio-diversity (Chao index of α diversity) of prokaryotic and eukaryotic microorganisms in Lake Basomtso sediments using high-throughput sequencing of sedaDNA.

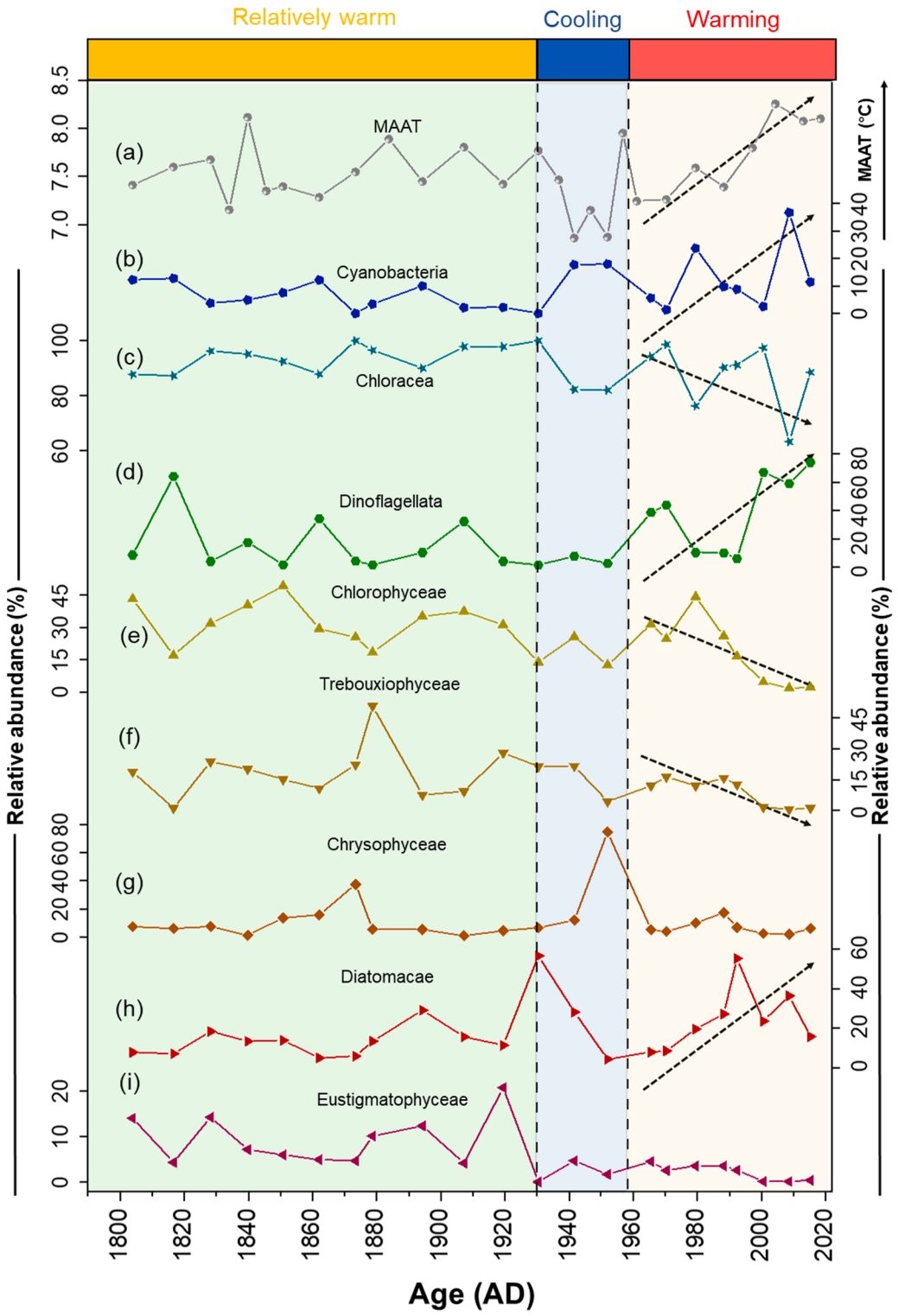

Fig. 6. Changes in the relative abundances of the photosynthetic microbial groups recovered in a sediment core from the Lake Basomtso with temperature over the past 200 yrs. (a) MAAT; the proportion of (b) *Cyanobacteria* and (c) *Chloracea* in the prokaryotic photosynthetic microorganisms; the proportion of (d) *Dinoflagellata*, (e) *Chlorophyceae*, (f) *Trebouxiophyceae*, (g) *Chrysophyceae*, (h) *Diatomacae*, (i) *Eustigmatophyceae* in Eukaryotic photosynthetic microorganisms.

since 1960 and the relative abundance of these three photosynthetic microorganisms shows a rising trend. As temperatures rise, *Cyanobacteria, Dinoflagellata,* and *Diatomacae* gain a competitive advantage and tend to flourish, and biodiversity increases significantly.

The evolution of the photosynthetic microbial community in Lake Basomtso is mainly due to climate change. On one hand, the increase in temperature increases the rate of enzymatic reaction of photosynthetic microorganisms, which is conducive to the reproduction of photosynthetic microorganisms and the increase in biomass (Huo et al., 2022a), For *Cyanobacteria* in particular, the increase in temperature will further enhance the competitive advantage of *Cyanobacteria* compared to other microorganisms (Carey et al., 2012). On other hand, rising temperatures

are expected to cause the meltdown of glaciers, which increases surface runoff and lead to increased nutrient input to lakes (Anslan et al., 2020). This has led to a shift in the microbial community of the lake. Similar climate-driven changes in microbial communities have also been identified in the Tibetan plateau at Yamdrok Yumtso (Huo et al., 2022a). It is worth noting that although Lake Basomtso is a glacial lake with less impact from human activities (Fig. S2) and low microbial diversity, the biodiversity of both eukaryotes and prokaryotes increased significantly, with the relative abundance of cyanobacteria increasing from 6% to 15.5%, and diatoms from 15.7% to 31.7%, respectively. The flourishing of these microorganisms and the increase in total number and diversity may be potentially harmful to the original lake ecosystem which is less resilient. The fragile ecosystems of glacial lakes are difficult to restore once contaminated, and therefore ecological monitoring and protection of these glacial lakes should be strengthened in the future.

4. Conclusions

This study reconstructed the temporal dynamics of temperature and photosynthetic microbial communities in Lake Basomtso on the Tibetan Plateau over the past two centuries. The MAAT at Lake Basomtso varied from 6.9 to 8.3 °C and rose rapidly after the 1950s, with MAAT remaining above 8 °C for the last two decades. Carbon isotope and *n*-alkane analyses indicate that the sediments were mainly derived from a mixed input of endogenous organic matter from terrestrial C_3 plants and photosynthetic microorganisms. After the 1960s, the contribution from endogenous organic matter in the sediments of Lake Basomtso gradually increased as the primary productivity within the lake continued to increase, mainly due to rising temperatures rather than increased anthropogenic nutrient input. *Chloracea* is by far the most dominant prokaryotic photosynthetic microbial community in Lake Basomtso, but the relative abundance of *Cyanobacteria* has increased significantly in recent years. Among the eukaryotic photosynthetic microbes, *Chlorophyceae* has now been replaced by *Dinoflagellata* and *Diatomacae*, despite having the highest average relative abundance, overall. Climate warming and its consequent glacial melting are the two main causes of the succession of photosynthetic microbial communities.

Our findings suggest that global warming has significant implications for glacial lake ecosystems on the Tibetan plateau. In the context of continued future warming, glaciers are expected to melt and retreat rapidly, bringing more additional nutrients to glacial lakes. The biomass and community composition of photosynthetic microbes are likely to increase dramatically. Given the fragility and importance of glacial lake ecosystems, more expeditions are urgently needed to understand the current state of water quantity and quality in highland glacial lakes globally, and how they will respond to rapid climate change. More extensive field station monitoring systems need to be built to obtain long-term, continuous monitoring data, which will enable us to better understand the resilience of highland glacial lakes and the extent to which our human activities impact these fragile yet important freshwater ecosystems.

Declaration of Competing Interest

The authors declare that they have no known competing financial interests or personal relationships that could have appeared to influence the work reported in this paper.

Data availability

Data will be made available on request.

Acknowledgments

This study was supported by the Strategic Priority Research Program of CAS (No. XDB40020400), the National Key R&D Plan of China (2021YFC3201000), the Central Leading Local Science and Technology Development Fund Project (20214028), the Science and Technology Service Plan of CAS (KFJSTSQYZD202124001), the National Natural Science Foundation of China (No. 41773145, 41977296, 42073072), and the Youth Innovation Promotion Association CAS (No. 2019389).

Supplementary materials

Supplementary material associated with this article can be found, in the online version, at doi:10.1016/j.watres.2023.120213.

References

Anslan, S., Rad, M.A., Buckel, J., Galindo, P.E., Kai, J.L., Kang, W.G., Keys, L., Maurischat, P., Nieberding, F., Reinosch, E., Tang, H.D., Tran, T.V., Wang, Y.Y., Schwalb, A., 2020. Reviews and syntheses: how do abiotic and biotic processes respond to climatic variations in the Nam Co catchment (Tibetan Plateau)? Biogeosciences 17, 1261–1279.

Appleby, P.G., Oldfield, F., 1978. The calculation of lead-210 dates assuming a constant rate of supply of unsupported ^{210}Pb to the sediment. Catena 5, 1–8.

Carey, C.C., Ibelings, B.W., Hoffmann, E.P., Hamilton, D.P., Brookes, J.D., 2012. Eco-physiological adaptations that favour freshwater cyanobacteria in a changing climate. Water Res. 46, 1394–1407.

Chen, X., Qiao, Q., McGowan, S., Zeng, L., Stevenson, M.A., Xu, L., Huang, C., Liang, J., Cao, Y., 2019. Determination of geochronology and sedimentation rates of shallow lakes in the middle Yangtze reaches using ^{210}Pb, ^{137}Cs and spheroidal carbonaceous particles. Catena 174, 546–556.

De Jonge, C., Hopmans, E.C., Stadnitskaia, A., Rijpstra, W.I.C., Hofland, R., Tegelaar, E., Sinninghe Damsté, J.S., 2013. Identification of novel penta- and hexamethylated branched glycerol dialkyl glycerol tetraethers in peat using HPLC-MS2, GC–MS and GC-SMB-MS. Org. Geochem. 54, 78–82.

Dong, J., Cui, X., Wang, S., Wang, F., Pang, Z., Xu, N., Zhao, G., Wang, S., 2016. Changes in biomass and quality of alpine steppe in response to N & P fertilization in the Tibetan Plateau. PLoS ONE 11, e0156146.

Feng, X., Zhao, C., D'Andrea, W.J., Liang, J., Zhou, A., Shen, J., 2019. Temperature fluctuations during the Common Era in subtropical southwestern China inferred from brGDGTs in a remote alpine lake. Earth Planet. Sci. Lett. 510, 26–36.

Ferrat, M., Weiss, D.J., Dong, S., Large, D.J., Spiro, B., Sun, Y., Gallagher, K., 2012. Lead atmospheric deposition rates and isotopic trends in Asian dust during the last 9.5 kyr recorded in an ombrotrophic peat bog on the eastern Qinghai-Tibetan Plateau. Geochim. Cosmochim. Acta 82, 4–22.

Ficken, K.J., Li, B., Swain, D.L., Eglinton, G., 2000. An *n*-alkane proxy for the sedimentary input of submerged/floating freshwater aquatic macrophytes. Org. Geochem. 31, 745–749.

Gast, R.J., Dennett, M.R., Caron, D.A., 2004. Characterization of protistan assemblages in the Ross Sea, Antarctica, by denaturing gradient gel electrophoresis. Appl. Environ. Microbiol. 70, 2028–2037.

Hugonnet, R., McNabb, R., Berthier, E., Menounos, B., Nuth, C., Girod, L., Farinotti, D., Huss, M., Dussaillant, I., Brun, F., Kaab, A., 2021. Accelerated global glacier mass loss in the early twenty-first century. Nature 592, 726–731.

Huo, S., Zhang, H., Wang, J., Chen, J., Wu, F., 2022a. Temperature and precipitation dominate millennium changes of eukaryotic algal communities in Lake Yamzhog Yumco, Southern Tibetan Plateau. Sci. Total Environ. 829, 154636.

Hopmans, E.C., Schouten, S., Sinninghe Damsté, J.S., 2016. The effect of improved chromatography on GDGT-based palaeoproxies. Org. Geochem. 93, 1–6.

Immerzeel, W.W., van Beek, L.P.H., Bierkens, M.F.P., 2010. Climate change will affect the Asian Water Towers. Science 328, 1382–1385.

Jia, W., Anslan, S., Chen, F., Cao, X., Dong, H., Dulias, K., Gu, Z., Heinecke, L., Jiang, H., Kruse, S., Kang, W., Li, K., Liu, S., Liu, X., Liu, Y., Ni, J., Schwalb, A., Stoof-Leichsenring, K.R., Shen, W., Tian, F., Wang, J., Wang, Y., Wang, Y., Xu, H., Yang, X., Zhang, D., Herzschuh, U., 2022. Sedimentary ancient DNA reveals past ecosystem and biodiversity changes on the Tibetan Plateau: overview and prospects. Quat. Sci. Rev. 293, 107703.

Kang, X., Song, J., Yuan, H., Duan, L., Li, X., Li, N., Liang, X., Qu, B., 2017. Speciation of heavy metals in different grain sizes of Jiaozhou Bay sediments: Bioavailability, ecological risk assessment and source analysis on a centennial timescale. Ecotoxicol. Environ. Saf. 143, 296–306.

Keck, F., Millet, L., Debroas, D., Etienne, D., Galop, D., Rius, D., Domaizon, I., 2020. Assessing the response of micro-eukaryotic diversity to the Great Acceleration using lake sedimentary DNA. Nat. Commun. 11, 3831.

Li, J., Lv, L., Wang, R., Long, H., Yang, X., 2022. Spatial distribution of *n*-alkanes in the catchment and sediments of Lake Lugu, Southwest China: implications for palaeoenvironment reconstruction. Palaeogeogr. Palaeoclimatol. Palaeoecol. 592, 110895.

Li, K., Liu, X., Wang, Y., Herzschuh, U., Ni, J., Liao, M., Xiao, X., 2017. Late Holocene vegetation and climate change on the southeastern Tibetan Plateau: implications for the Indian Summer Monsoon and links to the Indian Ocean Dipole. Quat. Sci. Rev. 177, 235–245.

Li, K., Liu, X.Q., Herzschuh, U., Wang, Y.B., 2016. Rapid climate fluctuations over the past millennium: evidence from a lacustrine record of Basomtso Lake, southeastern Tibetan Plateau. Sci. Rep. 6, 24806.

Lin, Q., Xu, L., Hou, J., Liu, Z., Jeppesen, E., Han, B.-P., 2017. Responses of trophic structure and zooplankton community to salinity and temperature in Tibetan lakes: implication for the effect of climate warming. Water Res. 124, 618–629.
Liu, C., Zhu, L.P., Wang, J.B., Ju, J.T., Ma, Q.F., Qiao, B.J., Wang, Y., Xu, T., Chen, H., Kou, Q.Q., Zhang, R., Kai, J.L., 2021. -situ water quality investigation of the lakes on the Tibetan Plateau. Sci. Bull. 66, 1727–1730.
Lu, X., Zhou, F., Chen, F., Lao, Q., Zhu, Q., Meng, Y., Chen, C., 2020. Spatial and seasonal variations of sedimentary organic matter in a subtropical bay: implication for human interventions. Int. J. Environ. Res. Public Health 17 (4), 1362.
Martin, C., Ménot, G., Thouveny, N., Peyron, O., Andrieu-Ponel, V., Montade, V., Davtian, N., Reille, M., Bard, E., 2020. Early Holocene Thermal Maximum recorded by branched tetraethers and pollen in Western Europe (Massif Central, France). Quat. Sci. Rev. 228, 106109.
Martínez-Sosa, P., Tierney, J.E., Stefanescu, I.C., Crampton-Flood, E.D., Shuman, B.N., Routson, C., 2021. A global Bayesian temperature calibration for lacustrine brGDGTs. Geochim. Cosmochim. Acta 305, 87–105.
McLauchlan, K.K., Williams, J.J., Craine, J.M., Jeffers, E.S., 2013. Changes in global nitrogen cycling during the Holocene epoch. Nature 495, 352–355.
Meyers, P.A., 2003. Applications of organic geochemistry to paleolimnological reconstructions: a summary of examples from the Laurentian Great Lakes. Org. Geochem. 34, 261–289.
Monchamp, M.-E., Spaak, P., Domaizon, I., Dubois, N., Bouffard, D., Pomati, F., 2018. Homogenization of lake cyanobacterial communities over a century of climate change and eutrophication. Nat. Ecol. Evol. 2, 317–324.
Mukai, H., Tanaka, A., Fujii, T., Zeng, Y.Q., Hong, Y.T., Tang, J., Guo, S., Xue, H.S., Sun, Z.L., Zhou, J.T., Xue, D.M., Zhao, J., Zhai, G.H., Gu, J.L., Zhai, P.Y., 2001. Regional characteristics of sulfur and lead isotope ratios in the atmosphere at several Chinese urban sites. Environ. Sci. Technol. 35, 1064–1071.
Murphy, J., Riley, J.P., 1962. A modified single-solution method for the determination of phosphate in natural waters. Analyt. Chim. Acta 27, 31–36.
Nübel, U., Garcia-Pichel, F., Muyzer, G., 1997. PCR primers to amplify 16S rRNA genes from cyanobacteria. Appl. Environ. Microbiol. 63, 3327–3332.
O'Beirne, M.D., Werne, J.P., Hecky, R.E., Johnson, T.C., Katsev, S., Reavie, E.D., 2017. Anthropogenic climate change has altered primary productivity in Lake Superior. Nat. Commun. 8, 15713.
Pepin, N., Bradley, R.S., Diaz, H.F., Baraer, M., Caceres, E.B., Forsythe, N., Fowler, H., Greenwood, G., Hashmi, M.Z., Liu, X.D., Miller, J.R., Ning, L., Ohmura, A., Palazzi, E., Rangwala, I., Schoener, W., Severskiy, I., Shahgedanova, M., Wang, M.B., Williamson, S.N., Yang, D.Q., Mt Res Initiative, E.D.W.W.G., 2015. Elevation-dependent warming in mountain regions of the world. Nat. Clim. Chang 5, 424–430.
Pinckney, J.L., Paerl, H.W., Tester, P., Richardson, T.L., 2001. The role of nutrient loading and eutrophication in estuarine ecology. Environ. Health Perspect. 109, 699–706.
Poynter, J.G., Farrimond, P., Robinson, N., Eglinton, G., 1989. Aeolian-derived higher plant lipids in the marine sedimentary record: links with palaeoclimate. In: Leinen, M., Sarnthein, M. (Eds.), Paleoclimatology and Paleometeorology: Modern and Past Patterns of Global Atmospheric Transport. Dordrecht, Springer Netherlands, pp. 435–462.
Ren, Z., Jiang, Z., Cai, Q., 2013. Longitudinal patterns of periphyton biomass in Qinghai-Tibetan Plateau streams: an indicator of pasture degradation. Q. Int. 313, 92–99.
Reuer, M.K., Boyle, E.A., Grant, B.C., 2003. Lead isotope analysis of marine carbonates and seawater by multiple collector ICP-MS. Chem. Geol. 200, 137–153.
Tan, H., Chen, J., Rao, W., Yang, J., Ji, J., Chivas, A.R., 2014. Lead isotope variability of fine-grained river sediments in Tibetan Plateau water catchments: Implications for geochemical provinces and crustal evolution. Lithos 190, 13–26.
Tang, S., Vlug, A., Piao, S., Li, F., Wang, T., Krinner, G., Li, L.Z.X., Wang, X., Wu, G., Li, Y., Zhang, Y., Lian, X., Yao, T., 2023. Regional and teleconnected impacts of the Tibetan Plateau surface darkening. Nat. Commun. 14, 32. -32.
Tao, S.L., Fang, J.Y., Ma, S.H., Cai, Q., Xiong, X.Y., Tian, D., Zhao, X., Fang, L.Q., Zhang, H., Zhu, J.L., Zhao, S.Q., 2020. Changes in China's lakes: climate and human impacts. Natl. Sci. Rev. 7, 132–140.
Tierney, J.E., Russell, J.M., Eggermont, H., Hopmans, E.C., Verschuren, D., Sinninghe Damsté, J.S., 2010. Environmental controls on branched tetraether lipid distributions in tropical East African lake sediments. Geochim. Cosmochim. Acta 74, 4902–4918.
Van de Peer, Y., De Rijk, P., Wuyts, J., Winkelmans, T., De Wachter, R., 2000. The European small subunit ribosomal RNA database. Nucleic Acids Res. 28, 175–176.
Watson, S.B., McCauley, E., Downing, J.A., 1997. Patterns in phytoplankton taxonomic composition across temperate lakes of differing nutrient status. Limnol. Oceanogr. 42, 487–495.
Williamson, C.E., Saros, J.E., Schindler, D.W., 2009. Climate change sentinels of change. Science 323, 887–888.
Wischnewski, J., Kramer, A., Kong, Z., Mackay, A.W., Simpson, G.L., Mischke, S., Herzschuh, U., 2011. Terrestrial and aquatic responses to climate change and human impact on the southeastern Tibetan Plateau during the past two centuries. Glob. Chang. Biol. 17, 3376–3391.
Xu, B.Q., Cao, J.J., Hansen, J., Yao, T.D., Joswia, D.R., Wang, N.L., Wu, G.J., Wang, M., Zhao, H.B., Yang, W., Liu, X.Q., He, J.Q., 2009. Black soot and the survival of Tibetan glaciers. Proc. Natl. Acad. Sci. U.S.A. 106, 22114–22118.
Yao, T., Thompson, L., Yang, W., Yu, W., Gao, Y., Guo, X., Yang, X., Duan, K., Zhao, H., Xu, B., Pu, J., Lu, A., Xiang, Y., Kattel, D.B., Joswiak, D., 2012. Different glacier status with atmospheric circulations in Tibetan Plateau and surroundings. Nat. Clim. Chang. 2, 663–667.
Yao, Y., Huang, Y.S., Zhao, J.J., Wang, L., Cheng, H., 2022. Lipid biomarkers in Lake Wudalianchi record abrupt environmental changes from the volcanic eruption in 1776. Org. Geochem. 164.
Zhan, C., Wan, D., Han, Y., Zhang, J., 2019. Historical variation of black carbon and PAHs over the last similar to 200 years in central North China: evidence from lake sediment records. Sci. Total Environ. 690, 891–899.
Zhang, G.Q., Bolch, T., Chen, W.F., Cretaux, J.F., 2021a. Comprehensive estimation of lake volume changes on the Tibetan Plateau during 1976-2019 and basin-wide glacier contribution. Sci. Total Environ. 772, 145463.
Zhang, H., Huo, S., Yeager, K.M., Wu, F., 2021b. Sedimentary DNA record of eukaryotic algal and cyanobacterial communities in a shallow Lake driven by human activities and climate change. Sci. Total Environ. 753, 141985.
Zhang, J., Shi, K., Paerl, H.W., Ruhland, K.M., Yuan, Y., Wang, R., Chen, J., Ge, M., Zheng, L., Zhang, Z., Qin, B., Liu, J., Smol, J.P., 2023a. Ancient DNA reveals potentially toxic cyanobacteria increasing with climate change. Water Res. 229, 119435.
Zhang, Q., Shen, Z., Pokhrel, Y., Farinotti, D., Singh, V.P., Xu, C.-Y., Wu, W., Wang, G., 2023b. Oceanic climate changes threaten the sustainability of Asia's water tower. Nature 615, 87–93.
Zheng, J., Tan, M.G., Shibata, Y., Tanaka, A., Li, Y., Zhang, G.L., Zhang, Y.M., Shan, Z., 2004. Characteristics of lead isotope ratios and elemental concentrations in PM10 fraction of airborne particulate matter in Shanghai after the phase-out of leaded gasoline. Atmos. Environ. 38, 1191–1200.
Zhu, T., Wang, X., Lin, H., Ren, J., Wang, C., Gong, P., 2020. Accumulation of pollutants in proglacial lake sediments: impacts of glacial meltwater and anthropogenic activities. Environ. Sci. Technol. 54, 7901–7910.